Analysis of urban heat island: a case study of Lecce, Italy

Author: Silvia Di Pietro[1]
Supervisors: Prof. Gianluca Pappaccogli[1]

[1] *Università del Salento*
E–mail: *silvia.dipietro@studenti.unisalento.it*

Abstract

This study aims to investigate the Urban Heat Island (UHI) phenomenon in the Mediterranean city of Lecce over a four-year period (2020-2023) and assess the potential impact of heatwaves on its intensity. Using temperature data collected from multiple urban and suburban sites, a comprehensive analysis to characterize the temporal patterns of UHI within the city was conducted. Additionally, heatwave events during the study period was identified and analyzed to examine their association with the exacerbation of UHI. The findings reveal significant diurnal and seasonal variations in UHI intensity across different urban settings, with higher UHI values observed during nighttime hours. Furthermore, a correlation between heatwave events and increased UHI intensity was observed, particularly during nighttime, indicating a potential amplification of UHI effects during extreme heat conditions. These results underscore the importance of understanding the interactions between heatwaves and UHI in Mediterranean urban environments and highlight the need for effective mitigation strategies to address the impacts of urban heat on public health and urban resilience.

Key words. Urban Heat Island – Heatwaves – Urban Cool Island – Mediterranean city

1. Introduction

Urban areas represent complex systems where morphological characteristics, such as building geometry and vegetation coverage, alongside physical properties of buildings and pavement materials, significantly influence mass, energy, and momentum fluxes within the urban canopy layer. Alterations in microclimatic conditions within this layer can affect thermal comfort [Zhou et al. (2020)] and air quality [Ordóñez et al. (2010)], leading to negative consequences on human wellbeing. Additionally, urban areas have experienced significant expansion in both size and density and the study of the Urban Heat Island (UHI) [Oke (1982)] phenomenon is crucial for understanding its impact on local climates and for informing effective mitigation strategies. The phenomenon of the urban heat island appears to be heightened [Li and Bou-Zeid (2013), Zhao et al. (2014), Tomlinson et al. (2012)]during prolonged periods of extreme heat, known as heatwaves, particularly recurrent during summertime.

The objective of this study, focused on a time period of 4 years in the city of Lecce, aims firstly to analyze the UHI phenomenon through the study of temperatures recorded at 5 different sites. Secondly, it seeks to determine the occurrence of heatwaves and assess their role in exacerbating the UHI effect.

2. Methodology

2.1. Study area

The area of interest is the city of Lecce, a medium sized city located in the central part of the Salentine Peninsula, within the southeastern Apulia Region of Italy. Lecce is situated on flat terrain, approximately 40–50 meters above sea level. According to the Köppen-Geiger classification, a widely used

system for quantifying world climates, Lecce falls into the Warm Mediterranean Climate 'Csa' category. This classification signifies a temperate-hot climate, characterized by an average temperature of the coldest month ranging between 6°C and 10°C, an annual average temperature between 14.5°C and 17°C, and at least four months with an average temperature exceeding 20°C [Gatto et al. (2021)].

2.2. Measurement sites

This study aims to evaluate the intensity of the Urban Heat Island effect and its amplification during heatwaves. Data recorded by six weather stations were analyzed for this purpose. For a detailed examination of the specific characteristics associated with each urban and suburban station, refer to Donateo et al. (2023). Table 1 presents an overview of the characteristics of the dataset considered in this study. The temperature dataset spans a period of four years, from 2020 to 2023, and covers data collected from five distinct weather stations situated within the city of Lecce, along with one station located in the nearby countryside. These weather stations provide measurements at regular intervals, with a time step of 30 minutes. The dataset includes information on various meteorological parameters, with a specific focus on near-surface air temperatures recorded at each station. The raw half-hourly data underwent preprocessing, which firstly involved applying a despiking procedure. These spikes were defined as absolute deviations from the mean exceeding six times the standard deviation within a month. Additionally, data gaps shorter than two hours were addressed using linear interpolation. To facilitate a comprehensive understanding of the study's outcomes, a brief description of the meteorological stations is provided below:

Urban stations

- Arpa: managed by the Environmental Protection Regional Agency of the Apulia region (ARPA-Puglia) and located on the ARPA building rooftop (13 m a.g.l.). It is located in the southern part of the city, mainly characterised by midrise buildings and separated by non-extensive and scattered green areas.

- Rudiae: operated by the Institute of Atmospheric Sciences and Climate (ISAC) of the Italian National Research Council (CNR). It is located on the roof of a historical building (12 m a.g.l), in the inner urban area.

- Ateneo: it is located 500 m apart from the Rudiae station. Both stations are contiguous to the historic centre, characterised by buildings made of calcareous tufa and streets paved with local stone (high heat capacity and heat conductivity.

- Liceo Scientifico Tabacchi, refered as Lecce in this study: is operated by the Civil Protection Agency of the Apulia region. This area is characterised in the northern part by large public (cemetery, equipped parks) and private green areas while compact low-rise buildings of residential use are in the south area.

Suburban station

- Isac: is located on the roof of the Institute of Atmospheric Sciences and Climate (ISAC) at 20 m a.g.l. This area is characterized by low building density and abundant vegetation.

Rural station

- Cerrate: managed by the Environmental Protection Regional Agency of the Apulia region (ARPA-Puglia), it is located in the countryside to the north of Lecce.

3. Results

3.1. Air temperature

The distribution of the data and its variability are shown in Fig. 1, which provides a compact summary of the central tendency, dispersion, and skewness of the hourly mean temperature observed across the six stations throughout the four-year period. Rudiae emerges as the site with the highest average temperature value, reaching 18.34 °C). the other urban stations exhibit temperature values spanning from 17.12 °C (Isac) to 17.85 °C (Lecce). Notably, the rural station of Cerrate consistently records the lowest average hourly temperatures, averaging 16.29 °C). The Arpa station stands out for registering the highest absolute temperature, peaking at 43.42 °C), while Isac is the one recording the absolute lowest temperature (-2.02 °C).

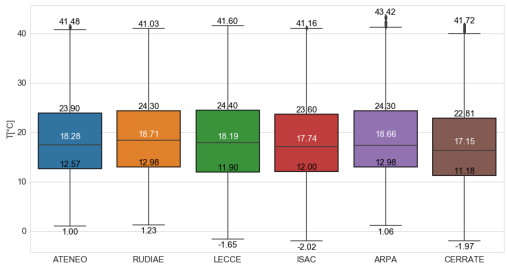

Fig. 1: Statistical analysis of hourly temperatures detected at the six stations from January 2020 to December 2023: maximum value, minimum value, first quartile, median, third quartile.

Table 1: Main characteristics of the weather stations.

Station	Coordinates (lat, lon)	Height a.g.l. (m)	Available Data	Temperature Available Data (%)
Arpa	40.345544°, 18.176957°	13	90363	82%
Ateneo	40.356172°, 18.167942°	11	105125	99%
Rudiae	40.351739°, 18.165027°	12	65330	56%
Lecce	40.359497°, 18.167669°	2	78538	62%
Isac	40.335820°, 18.124488°	20	103860	98%
Cerrate	40.458967°, 18.116311°	4	99465	98%

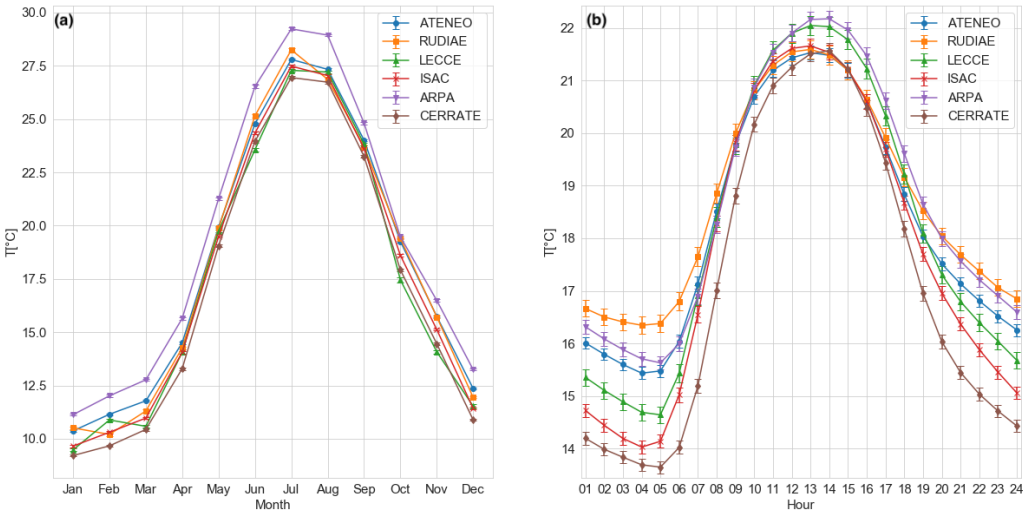

Fig. 2: Mean monthly and mean hourly of the air temperature. Error bars represent the standard error.

In Fig. 2(a), the monthly mean air temperature values for each station are depicted. July emerges as the month with the highest average temperature, whereas January exhibits the lowest. Arpa station consistently records the highest average monthly temperature across all months, with values ranging from 11.13 °C (in January) to 29.23 °C (in July). Conversely, the other urban stations, compared to Arpa station, display slightly cooler temperatures, ranging from 0.07 °C to 2.9 °C lower compered to Arpa. In Fig. 2(b) , the characteristic daily temperature patterns are illustrated. It is evident that the highest temperatures were consistently observed between 12:00-14:00 LT (LT=UTC+1) across all stations. Arpa and Lecce stations exhibited the highest averaged values, measuring 22.17 °C and 22.05 °C respectivelly,, respectively, while the remaining stations displayed temperatures of comparable magnitude, averaging 21.58 °C±0.072 °C.

Table 2 reports the warming and cooling rates computed based on hourly temperature data. the most pronounced warming and cooling rates are observed at the Lecce urban station and the Isac suburban station, which are comparable to those observed at the rural station of Cerrate. Conversely, Rudiae exhibits comparatively lower rates of both warming and cooling.

Table 2: Warming and cooling rates [$^{\circ}Ch^{-1}$]

Station	Warming Rate	Cooling Rate
Ateneo	0.67	0.36
Rudiae	0.58	0.30
Lecce	0.82	0.47
Isac	0.83	0.46
Arpa	0.69	0.42
Cerrate	0.84	0.49

3.2. Urban Heat Island Intensity UHII

The Urban Heat Island effect, marked by elevated temperatures within urban areas compared to their rural surroundings, constitutes a fundamental aspect of contemporary urbanization studies. To thoroughly investigate this phenomenon, it is imperative to conduct comparative analyses utilizing data from urban stations sharing similar topographical characteristics. The selection of stations with comparable topography ensures a more precise evaluation of temperature disparities associated with urbanization, thus mitigating the influence of geographical variations. The evaluation of urban heat island intensity (UHII) depends on the computation of the hourly-averaged air temperature difference between two stations: one located in the urban core and the other positioned in rural surroundings, as shown in the formula

$$UHII = T_{urb} - T_{rur}$$

where T_{urb} denotes the temperature recorded at the urban or suburban station, while T_{rur} represents the temperature measured at the rural station (Cerrate in this study).

3.2.1. UHII seasonal characterization

Table 3 presents the mean values of UHII categorized by season.The winter months (DJJ: December, January, February) and spring months (MAM: March, April, May) indeed show higher average UHII values, reaching 1.12 and 1.06 on average, respectively. However, the peak UHII value is observed during the summer months (JJA: June, July, August) at the Arpa station. These findings align with those previously observed in Donateo et al. (2023). Conversely, lower UHII values are prevalent during the summer months across most stations, with the Lecce station reporting the minimum value of 0.37°C.

Table 3: Seasonal average UHII [°C]

Station	DJF	MAM	JJA	SON
Ateneo	1.36	1.13	0.77	1.12
Rudiae	1.04	0.82	0.49	0.78
Lecce	0.54	0.55	0.37	0.47
Isac	0.51	0.54	0.44	0.54
Arpa	2.14	2.23	2.33	2.16

3.2.2. UHII diurnal characterization

Fig. 3 shows the hourly diurnal pattern for UHII averaged over the four-year period. The UHII displays a consistent trend across all stations. Each station exhibits maximum UHII values during the early morning hours (06:00-07:00), except for Arpa, where maximum UHII values occur between 20:00 and 24:00. Following the morning peak, there is a decline in UHII throughout the daytime hours before it rises again in the evening due to the release of infrared radiation from the urban area at sunset, persisting throughout the night. Lecce and Isac are characterized by recording the lowest average UHII values, aligning with previous studies Donateo et al. (2023) and reflecting their locations in areas with less dense urban development. The majority of stations demonstrate positive hourly average UHII values, delineating a distinct urban-rural temperature gradient. Conversely, the Rudiae station presents negative UHII values during midday hours, with a notable minimum average value of -0.85 recorded at 14:00.

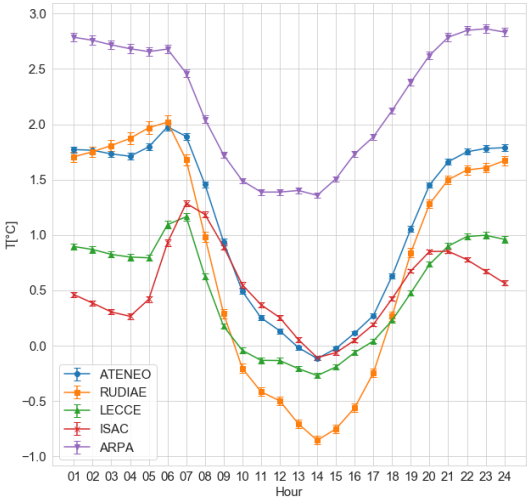

Fig. 3: Hourly diurnal pattern for UHII [°C] from January 2020 to December 2023. Error bars represent the standard error.

Fig. 4 shows the hourly average intensity of UHII [°C], computed for each month, over the four-year period. Upon analyzing obtained results, a comparison can be drawn regarding similarities and differences with the findings presented in Donateo et al. (2023).

- Ateneo (Fig. 4a): is reaffirmed as the station exhibiting a pattern more closely associated with that of UHII. It is characterized by significant temperature differences during the night (2-2.8 °C) and negative differences observed during the daytime. Notably, there is a discernible negative fluctuation in the intensity of UHII during the central hours of the days, observed between May and August.
- Rudiae (Fig. 4b): exhibits a UHII pattern very

similar to that of the Ateneo station, where it is more pronounced during spring and summer nights. However, unlike Ateneo, it shows the formation of a more intense urban cool (UCI) island, with mean negative values throughout the year and an intensification from April to August. The co-existence of UCI during the day and UHI at night has been previously documented in other cities [Yang et al. (2016)].

- Lecce (Fig. 4c): exhibits a weaker formation of UHI primarily observed during the nights from April to August (1.2-1.5 °C in May), with higher values registered during the early hours of the day (06:00-07:00 LT). Furthermore, negative UHII values are registered during the central hours of the day within the same annual range, with values comparable to those recorded by the Ateneo station and slightly lower than those characterizing the identified urban cool island of Rudiae.

- Isac (Fig. 4d): exhibits a behavior closely resembling that of Lecce. However, it exhibits annual UHI values that are less intense (both positive and negative), but with more pronounced intensity during the early hours of spring and summer days.

- Arpa (Fig. 4e): as previously detailed in Donateo et al. (2023), a consistent trend emerges with uniformly positive UHII values (also grater than 3°C during summer nights). As previously observed in other stations, lower UHII values are recorded during the central hours of the day a trend that remains consistent throughout a significant portion of the year.

3.3. Impact of Heat Waves on UHII

3.3.1. Temporal characteristics of heatwaves

To discern the impacts of UHI from broader climatic factors, a rigorous analysis was conducted to isolate heatwaves and their specific contributions to the Urban Heat Island Intensity .

Various definitions of heatwaves exist, often relying on daily maximum or minimum temperatures. In this study, the criteria set by Fischer and Schär (2010) is followed: a heat wave is defined as a period lasting at least six consecutive days during which the daily maximum temperature exceeds the 90th percentile of a reference period (1991-2020). Fig. 5 shows all the heatwaves identified during the referenced period, with color denoting the maximum temperatures recorded each day. Further details can be found in Table 4.

Throughout the analysis period, a total of 11 heatwaves were identified, with an average duration of 10 days and a maximum duration of 17 days observed between June and July of 2022. Remarkably, the year 2022 exhibited the longest-lasting heatwaves, spanning 17, 11, and 8 days, respectively, occurring between June 21st and August 9th, with an average temperature of 34.25°C. In the subsequent year of 2023, three heatwaves were recorded, with an average duration of 10 days and an average temperature of 35.9°C. Similarly, in 2022, there were also 3 heatwaves, with durations and average temperatures comparable to those of 2023 (9.6 days on average and 35.8°C on average). Conversely, in 2020, only 2 heatwaves were recorded, with shorter duration and lower intensities (lasting 7 days each and 33.4°C on average).

Table 4: Heatwaves Characteristics

Year	N°	Start	Stop	HWD n°day	HWA °C
2020	1	26/06	03/07	7	33.36
	2	29/07	04/08	7	33.43
2021	1	21/06	26/06	6	37.22
	2	25/07	05/08	12	36.60
	3	07/08	17/08	11	34.15
2022	1	21/06	07/07	17	34.56
	2	21/07	31/07	11	34.44
	3	02/08	09/08	8	33.35
2023	1	11/07	26/07	16	37.62
	2	28/07	04/08	8	33.96
	3	21/08	28/08	8	34.47

HWD: heatwave duration (number of days)
HWA: averaged temperature (°C)

3.3.2. Impact of heatwaves on Urban Heat Islands

Table 5 shows the summer seasonal (JJA) average of UHII, distinguishes between normal periods, which include occurrences of heatwaves (JJA HW), and periods without heatwaves (JJA NHW) for each station, along with their respective variations (Δ UHII). Of particular significance is the observation that Isac and Lecce, stations characterized by relatively lower levels of urbanization, demonstrate minimal variability.

To gain deeper insights into the influence of heatwaves on the urban heat island phenomenon, a more detailed analysis was conducted. This analysis focused on the following aspects: the hourly variation in urban heat island intensity and the distribution of maximum hourly values of urban heat island intensity.

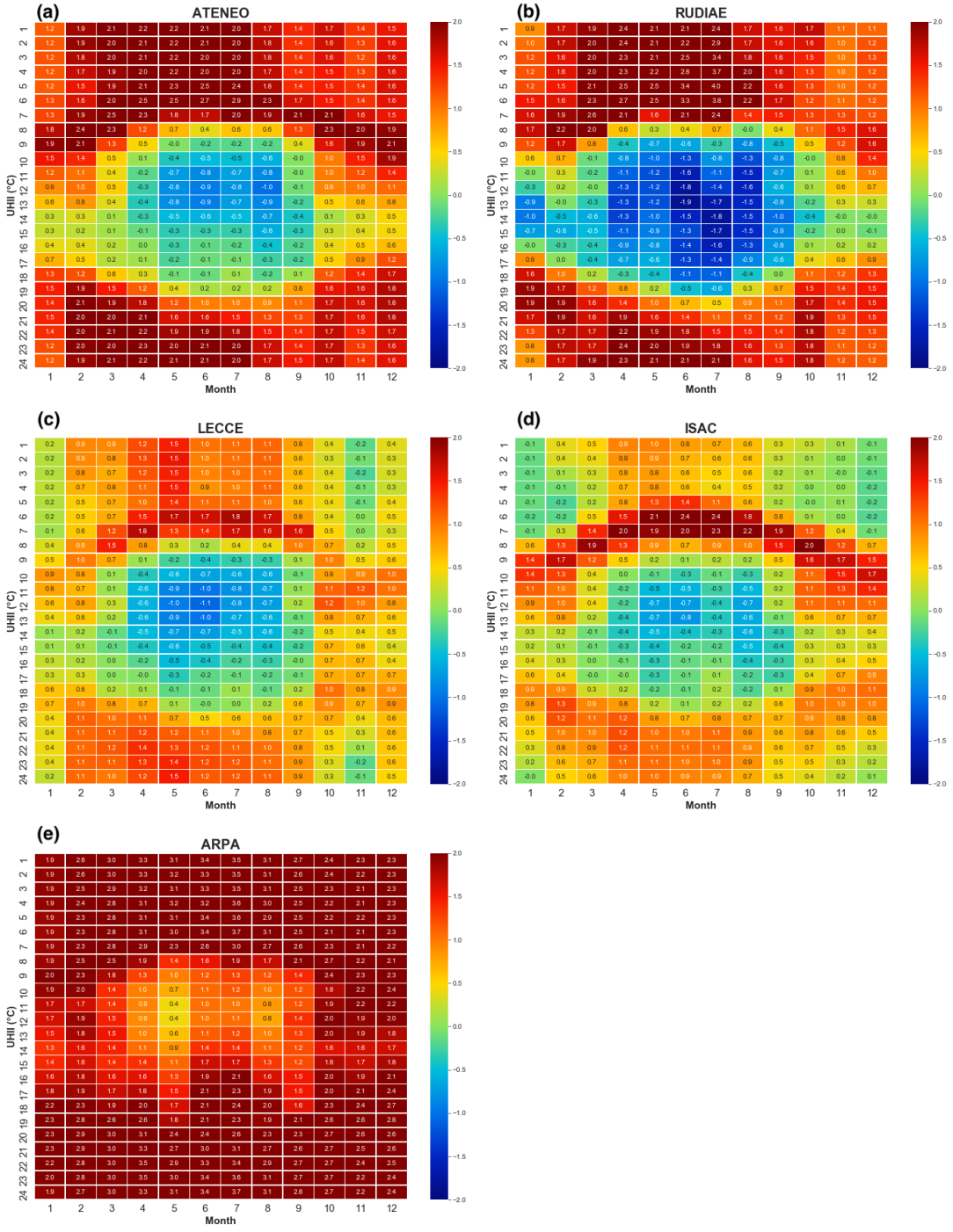

Fig. 4: Hourly diurnal pattern for UHII [°C] from January 2020 to December 2023.

3.3.3. UHII variation

Fig. 6(a-e) shows the hourly diurnal pattern of UHII during summer seasons, examining both conventional periods and those unaffected by heatwaves. Insights from this results reveal that all stations exhibit a slight increase in UHII when periods characterized by heatwaves are considered in the analysis. Particularly notable is the elevation of UHII during nighttime hours and in the midday hours. The anomalous behavior of the Rudiae station can be attributed to the lack of validated data during the summer period between 2020 and 2024.

Fig. 6(f) shows the differences in diurnal varia-

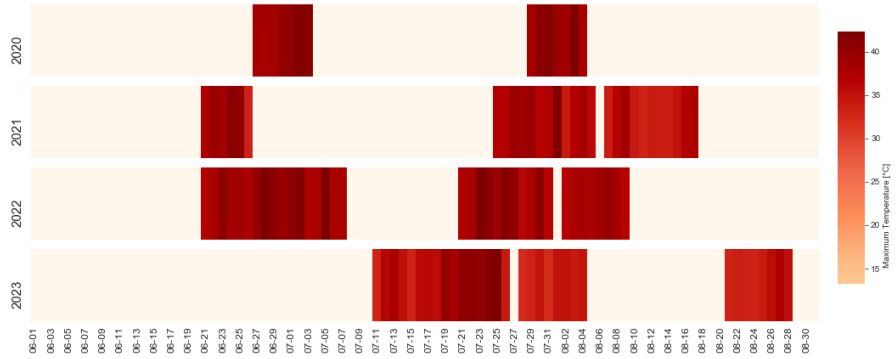

Fig. 5: A daily overview of heat waves and their intensity in the period 2020–2024 from 1 June to 31 August. Only days in heat waves are colored based on the highest daily air temperatures recorded.

Table 5: Average UHII [°C] in JJA season with and without heatwaves

Station	JJA HW	JJA NHW	Δ UHII
Ateneo***	0.77	0.61	0.16
Rudiae*	0.49	0.23	0.26
Lecce**	0.37	0.22	0.15
Isac**	0.44	0.29	0.15
Arpa***	2.33	2.07	0.26

* 56% of verified data in JJA HW
** up to 73% of verified data in JJA HW
*** up to 97% of verified data in JJA HW

tion of UHII in Heatwave (HW) and Non-Heatwave (NHW) periods. With the exception of Rudiae and ISAC stations, all stations exhibit a significant increase in Δ UHII during nighttime hours and a less pronounced yet still positive growth during daytime hours, suggesting an amplification of UHII due to heatwaves. The ISAC station, situated in a suburban area, displays more pronounced variations in ΔUHII) only during the early morning hours (06:00-08:00) and midday hours (11:00-13:00), with nearly identical UHII values during nighttime hours.

Fig. 7 shows the seasonal distribution of the hourly diurnal maxima of the UHII, specifically highlighting the difference between summer seasons considering both Heatwave (HW) periods and Non Heatwave (NHW) periods. Considering the seasonal distributions, peaks of frequency are observed in almost all stations for UHII values ranging between 1°C and 3°C in all seasons. Arpa demonstrates a higher percentage of frequencies for UHII values ranging between 3°C and 5°C, especially during the summer period, as previously discussed in Donateo et al. (2023). As expected, focusing solely on the summer season reveals a more or less pronounced decrease in the frequency of higher UHII values across all stations, accompanied by a corresponding increase in the frequency of lower UHII variations. This trend further underscores the significant impact of heatwaves on this phenomenon.

4. Conclusions

This study undertakes a comprehensive evaluation of the potential interactions between extreme heat events and the urban heat island phenomenon. The main outcomes reveal that:

- The urban heat island effect exhibits a consistent diurnal cycle across all analyzed stations, with higher UHI values observed during the nighttime hours in urban areas.
- For the Rudiae station, a coexistence of the urban heat island phenomenon during nighttime hours and the urban cool island phenomenon during daytime hours has been observed.
- During the period spanning from 2020 to 2023, a total of 11 heatwaves were detected, with the most prolonged one observed in 2022.
- Differences between diurnal and nocturnal Urban Heat Island Intensity are noticeable. Specifically, during nighttime, the UHII is higher on HW compared to NHW days.

Future work could focus on:

- Investigating the relationship between wind speed and direction and UHII to better understand the mechanisms driving UHII variations.
- Exploring the effectiveness of heatwave mitigation strategies, such as the implementation of cool roofs and the integration of green spaces.

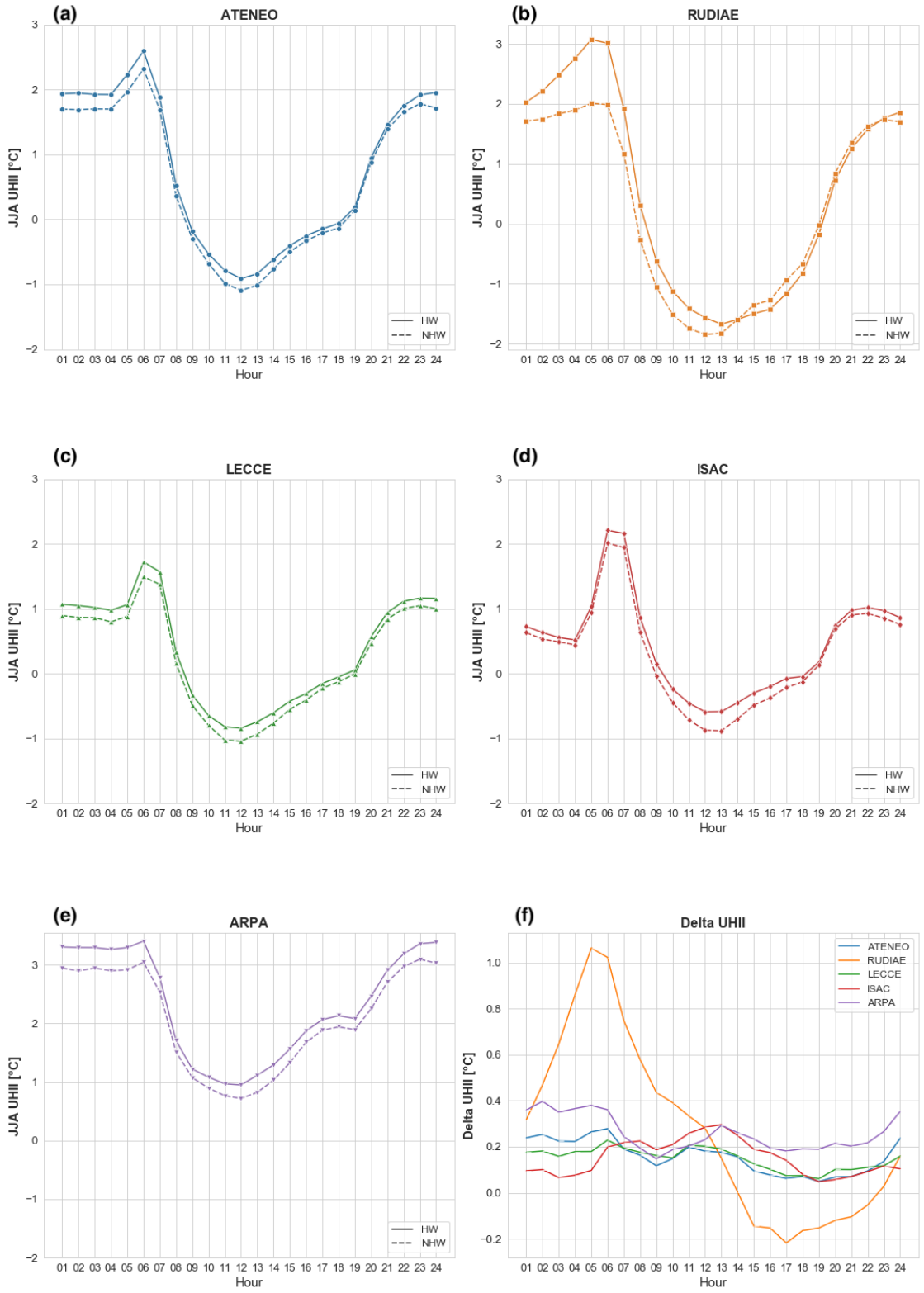

Fig. 6: Diurnal variation in UHII during HW and NHW periods in summer seasons (JJA) 2020-2023. Diurnal variation in UHII difference (Δ UHII) between HW and NHW periods in JJA season.

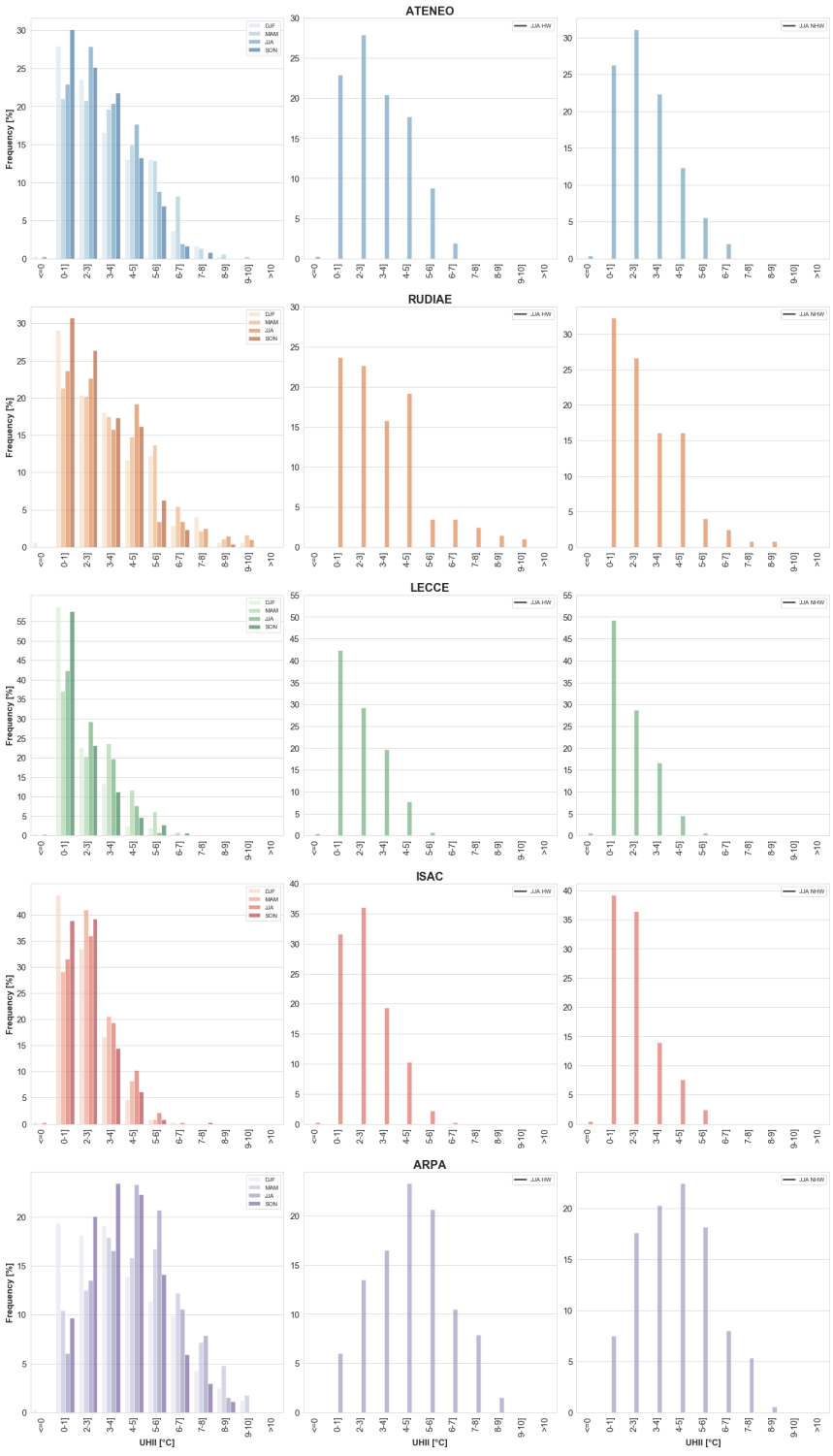

Fig. 7: Seasonal distribution of daily values of maximum hourly difference of temperature recorded during each day ($UHII_{max}$). Seasonal distribution of daily values of maximum hourly difference of temperature recorded during HW and NHW periods in summer seasons (JJA) 2020-2023.

REFERENCES

Donateo, A., Palusci, O., Pappaccogli, G., et al. 2023, Sustainable Cities and Society, 98, 104849

Fischer, E. M. and Schär, C. 2010, Nature Geoscience, 3, 398

Gatto, E., Ippolito, F., Rispoli, G., et al. 2021, Climate, 9

Li, D. and Bou-Zeid, E. 2013, Journal of applied Meteorology and Climatology, 52, 2051

Oke, T. R. 1982, Quarterly journal of the royal meteorological society, 108, 1

Ordóñez, C., Elguindi, N., Stein, O., et al. 2010, Atmospheric Chemistry and Physics, 10, 789

Tomlinson, C., Chapman, L., Thornes, J., and Baker, C. 2012, International Journal of Climatology, 32, 214

Yang, A. X., Li, Y., Luo, Z., and Chan, P. 2016, International Journal of Climatology, 37

Zhao, L., Lee, X., Smith, R. B., and Oleson, K. 2014, Nature, 511, 216

Zhou, X., Carmeliet, J., Sulzer, M., and Derome, D. 2020, Applied Energy, 278, 115620